ANALYTICAL SCIENCE & TECHNOLOGY
(Journal of the Korean Society of Analytical Sciences)
Vol. 8, No. 4, 1995
Printed in the Republic of Korea

In Situ Scanning Tunneling Microscope of Cyanide and Thiocyanate Adsorption on Pt(111)

Shueh-Lin Yau, Youn-Geun Kim, and Kingo Itaya*

Itaya Electrochemiscopy Project, ERATO/JRDC, Research Institute of Electric and Magnetic Materials, Sendai 982, Japan

**Faculty of Engineering, Tohuku University, Sendai, Japan 982*

Abstract: Cyclic voltammetry and in situ STM were employed to examine the interfacial structures of a Pt(111) electrode in 0.1 mM KCN (pH9.5) and 0.1 mM KSCN (pH7) solutions. In situ STM atomic resolution revealed well ordered $(2\sqrt{3}\times2\sqrt{3})R30°$-6CN and (2×2)-2SCN structures within the double layer charging region. Six CN adsorbates formed a hollow hexagon, which embraced a coadsorbed K^+ cation. In contrast, the coadsorbed K^+ cations on the SCN covered Pt(111) were poorly ordered, despite adsorbed SCN formed a long range ordered (2×2)-2SCN adlattice. In situ STM revealed the pronounced influence of potential in controlling the structures of compact layers at the proximity of a Pt electrode. Cathodic polarization facilitated the replacement of the coadsorbed cations by protons.

Keywords : In situ scanning tunneling microscopy, Pt(111) single crystal electrodes, cyanide and thiocyanate adsorption

1. Introduction

The well-established in situ scanning tunneling microscopy (STM) has extensively been employed to determine structures and structure changes of bare electrode surfaces such as single crystal Pt, Au, and Ag in electrolyte solutions.[1] The atomic structures of adlayers of halides such as I^-,[2,3] and Br^-,[4] or other inorganic ionic species such as CN^-,[5] and sulfate/bisulfate[6] have been investigated. This STM technique has brought significant impacts to electrochemistry for the elucidation of the nature of electrode/electrolyte interfaces at an atomic level.[8] The adlayers described above are thought to be directly bonded to the electrode surface. According to electrical double layer theory for the electrode/electrolyte interface, the above mentioned work have indeed unfolded detailed structural information of inner Helmholtz double layers which are composed of specifically adsorbed species including halides, sulfate/bisulfate, and water molecules.[7] However, to our knowledge, no in situ STM investigation has previously been carried out for the elucidation of details of outer Helmholtz plane (OHP). However, it is noteworthy that the adsorption of cations on top of the adlayers of halides, CN^-, and SCN^- formed on Pt single crystal electrodes has been intensively investigated by Hubbard and coworkers using an ex situ ultrahigh vacuum-electrochemical system.[8-10] It was reported that cations such as Li^+, Na^+, K^+, Cs^+, Ca^{2+}, Ba^{2+} and La^{3+} could be adsorbed on the well-defined CN and SCN adlayers on Pt(111).[10] Detailed structural information of the CN and SCN adlayers on Pt electrodes was also investigated by ex situ LEED[8-10] as well as in situ infrared spectroscopy (IR),[11-14] sum frequency generation,[15] and STM.[5] It is believed that the adsorbed CN and SCN linearly bind to the Pt substrate predominantly through their C- and S-ends, respectively. In situ STM was used to examine the strongly adsorbed CN and SCN adlayers on Pt(111). We also demonstrate here that in situ STM imaging could reveal the coadsorbed cations at the OHP.

2. Experimental

A Pt single crystal bead (3 mm in diameter) was made at one end of a pure Pt wire (1 mm in diameter). The well-prepared Pt bead consisted of (111) facets in an octahedral configuration. These (111) facets usually gave well defined terraces and steps structures, as shown in **Fig. 1**.[16] For voltammetric measurements, the Pt (111) single crystal was mechanically exposed with successive finer grade Al_2O_3 from 2 μm to 0.05 μm. The orientation of the single crystal was determined with a laser diffraction technique. The Pt (111) electrode was finally annealed by a H_2/O_2 flame for at least 3 hrs to remove surface damages caused by mechanical polishing. A flame-annealing and quenching procedure was used to expose the well-defined (111) surface into solution. The anneal-quenching was done in a hydrogen saturated Millipore water after its glowing color has disappeared in a H_2 stream. The cyclic voltammogram (CV) for the Pt(111) electrode in 0.1 M $HClO_4$ showed consistently the characteristic butterfly feature,[16,17] indicating that the well-ordered Pt(111) was successfully prepared by the procedure described above.

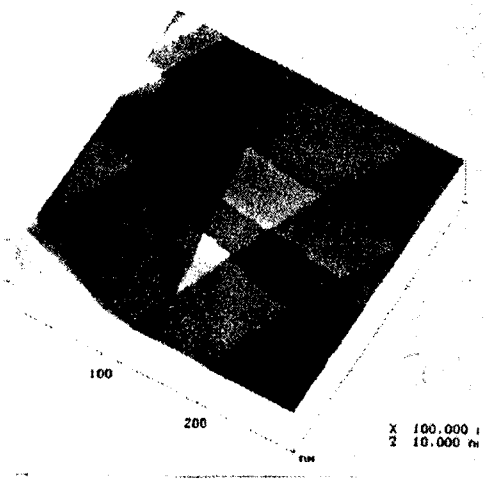

Fig. 1 A topographic scan of Pt(111) in 0.1 mM KSCN and 0.1 M $KClO_4$ (pH7).

Ultrapure KCN, KSCN and $NaClO_4$ were obtained from Ciga Merk Chemicals, and Millipore water was used to prepare all the solutions. NaOH and KOH solutions were used to adjust the pH of solutions to 9.5. The cyclic voltammetry was performed in an electrochemical cell with three compartments, including a reversible hydrogen reference electrode (RHE) either in pure electrolyte solutions of 0.1 M $HClO_4$ or 0.1 M $NaClO_4$ (pH= 9.5) in the absence of cyanide. A saturated calomel electrode (SCE) was also used to calibrate RHE in the different pH solutions. A Pt wire was used as a counter electrode. The potential was controlled by a Hokuto potentiostat (Tokyo, Japan). The STM was a NanoScope III STM (Digital Instruments, Santa Barbara, CA) was used with a modified STM cell employing the hydrogen reference electrode and Pt counter electrodes. The tip was a W wire (0.03 in) electrochemically etched in a 1 M KOH bath. The W tips were further painted with transparent nail polish to minimize the faradaic current.

3. Results and Discussion

3.1 Voltammetry of Pt(111) in Alkaline Cyanide and Thiocyanate Solutions. Figures

2(a) shows the typical steady-state CV for Pt(111) in 0.1 M $NaClO_4$ (pH9.5). The electrode potential is shown with respect to both reference electrodes of RHE (lower scale) and SCE (upper scale). The broad reversible wave at 0.85 V vs. RHE is probably due to the adsorption and desorption of perchlorate anions on Pt(111).[18,19] An irreversible oxidation peak at 1.3 V was interpreted as the adsorption of hydroxide (-OH) species on Pt(111). After this CV was recorded, the clean Pt(111), protected by a water layer, was then transferred to CN^- or SCN^- containing solutions. Firstly, **Fig. 2(b)** shows that the presence of CN^- in the solution eliminates the characteristic reversible peak of Pt(111) at 0.85 V and the irreversible oxidation peak at 1.1 V. A featureless double layer charging region extends from 0.3 to 1 V. It is also noticed that the characteristic hydrogen adsorption and desorption peaks are almost completely eliminated in the presence of CN^-. A reduction peak can be found at 0.1 V near the onset of the hydrogen evolution reaction. This might be due to a partial desorption of the adsorbed CN^- and to the adsorption of hydrogen simultaneously. This pronounced feature did not appear for poly Pt electrodes.[18] The CV shown in the dotted line in Fig. 2(b) was recorded with a fourfold increased current scale. It is found that a broad anodic peak at 0.62 V appears to be irreversible at the scan rate of 50 mV/s.

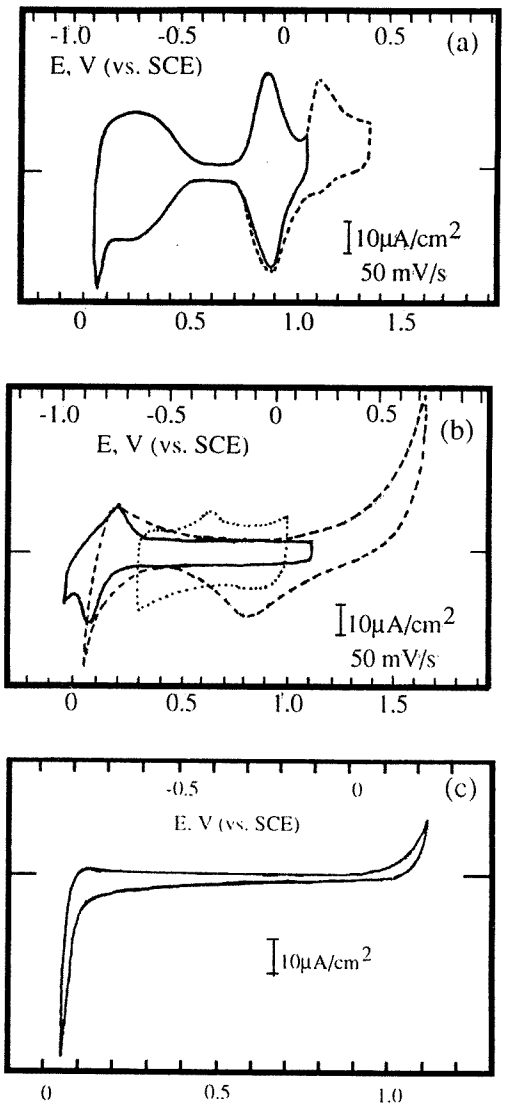

Fig. 2 Cyclic voltammograms of Pt(111) in 0.1 M $KClO_4$ (pH9.5) (a), 0.1 mM KCN, 0.1 M $KClO_4$ (b), and 0.1 mM KSCN, 0.1 M $KClO_4$ (pH7) (c). Scan rate; 50 mV/s.

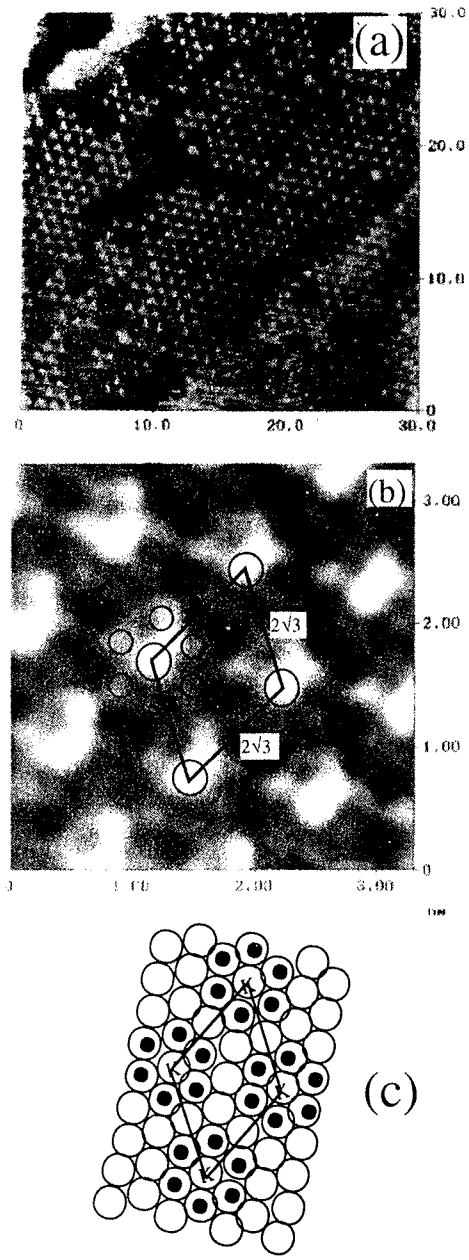

Fig. 3 (a) In situ STM atomic resolution of the Pt(111)-(2√3×2√3)R30°-KCN structure (b) A close-up of this 2√3 structure. (c) A ball model. The image was obtained at 0.6 V with a bias voltage of 100 mV and a feedback current of 5 nA.

It will be discussed in a later section that this peak is expected to be associated with the complexation of alkali cations such as Na^+ and K^+ with the CN adlayer. The dotted line in Fig. 2(b) was obtained after the potential was scanned to more positive than 1.5 V. The Pt(111) electrode is now rough and the CV characteristics are evidently different from those of a well-defined Pt(111) electrode. The CV for a Pt(111) electrode immersed in 0.1 mM KSCN (**Fig. 2(c)**) resembles that of CN but a precipitous increase of the anodic current commences at a much less positive potential. No cathodic feature emerges before the occurrence of hydrogen evolution. A possible oxidation reaction for SCN was proposed to yield SO_4^{2-} and CN^- whereas oxidation of CN predominantly produces CO_2.

3.2 Atomic STM Imaging in Alkaline KCN Solutions. The STM image shown in **Figure 3(a)** was obtained at 0.6 V in a 0.1 mM KCN + 0.1 M $KClO_4$ (pH9.5) solution. A long range (30x30 nm) ordered hexagonal pattern is immediately identified. The nearest neighbor distance of 0.096 nm is in good agreement with the lattice constant of the $(2\sqrt{3}\times2\sqrt{3})R30°$ structure. A close-up in **Fig. 3(b)** further reveals the details of this $2\sqrt{3}$ adlattice, which shows that the brighter center spot are actually surrounded by six weak protrusions. The corrugation amplitude of each center bright spot is ca. 0.035 nm. A ball model (**Fig. 3(c)**) for the CN adlayer can be constructed to reconcile the STM results; however, different registries of the CN adsorbates cannot explain the relatively higher corrugation of the center spots because they all occupy similar type of binding sites. Thus, we recall that the CN adlayer is anionic and one can expect the presence of coadsorbed cations such as K^+ in our present study. The brighter central spots are then likely attributed to the coadsorbed K^+ on the CN adlayer. It is interesting to note this complexation configuration resembles that of well-known crown ether for the alkali metal cations. Indeed, in situ STM imaging revealed the relative high mobility of the Na^+ cations with respect to K^+ so that higher quality STM results were readily obtained for the latter, but difficult for the former. This result resembles the well-known fact that K^+ binds 18-crown-6 stronger than Na^+ does. The relative large cavity size of 0.56 nm for our present CN adlattice implies that the retained cations could be in their hydrated states.

It is noted that a small hump appears at 0.6 V in the CV (dotted line in Figure 1(b)). We then try to use in situ STM to probe the surface processes occurring at this potential. The STM experiments were carried out firstly at 0.6 V, the peak of the CV feature. After nice STM results such as Fig. 3(a) were obtained at 0.6 V, the potential was stepped negatively to 0.5 V, which marks the foot of the CV feature at 0.6 V. It was found that K^+ ions, coordinating on ca. 90 % of the hexagonal rings at the potential of 0.6 V, were rapidly diminished, as shown by the STM image in **Fig. 4**. This STM image represents the stable surface state. The vanishing rate of K^+, however, sharply decreased, and it took a quite long time to eliminate all K^+. The coverage of K^+ became to be less than 10% after 16 min. The exchange rate seems to be controlled by the diffusion of hydronium cations. The slow vanish of K^+ is expected to be due to a consequence of the low concentration of protons in pH9.5 solution. On the other hand, stepping the potential of Pt positively

from 0.5 to 0.6 V readily recovered the ordered $2\sqrt{3}$ pattern of the adsorbed K^+ cations within 2 min. The above results have been described in detail in our recent paper.[21]

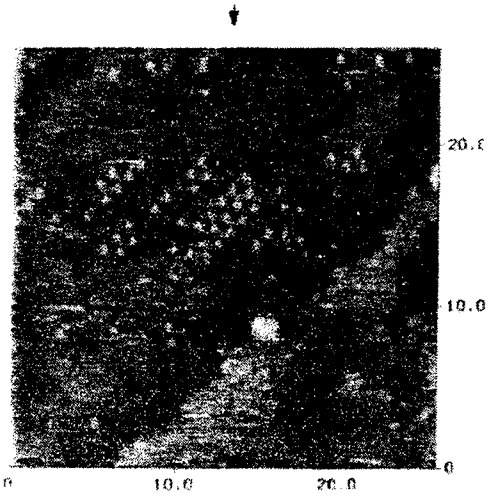

Fig. 4. An in situ STM image of CN on Pt(111) at 0.5 V. This image was obtained 16 min after the Pt potential was stepped to 0.5 V from Fig. 3(a)

3.3 In situ STM of SCN on Pt(111). Fig. 5(a) to **5(c)** present the potential dependence of the in situ STM images of a SCN covered Pt(111) electrode. The potential of the tip electrode was stepped together with the Pt electrode during the STM imaging. First of all, in situ STM reveals some local (2×2) structure at the open-circuit potential of 0.9 V (**Fig. 5(a)**). We experienced certain instability in the STM imaging and unknown blotches were frequently found. The best STM results could be obtained with a bias voltage of -160 mV and 2 nA feedback current. Once the potential of the Pt electrode was stepped negatively from 0.9 to 0.7 V, in situ STM unveiled an instant change of the surface. The Pt electrode was no longer uniform as shown by Fig. 5(a) and its surface became

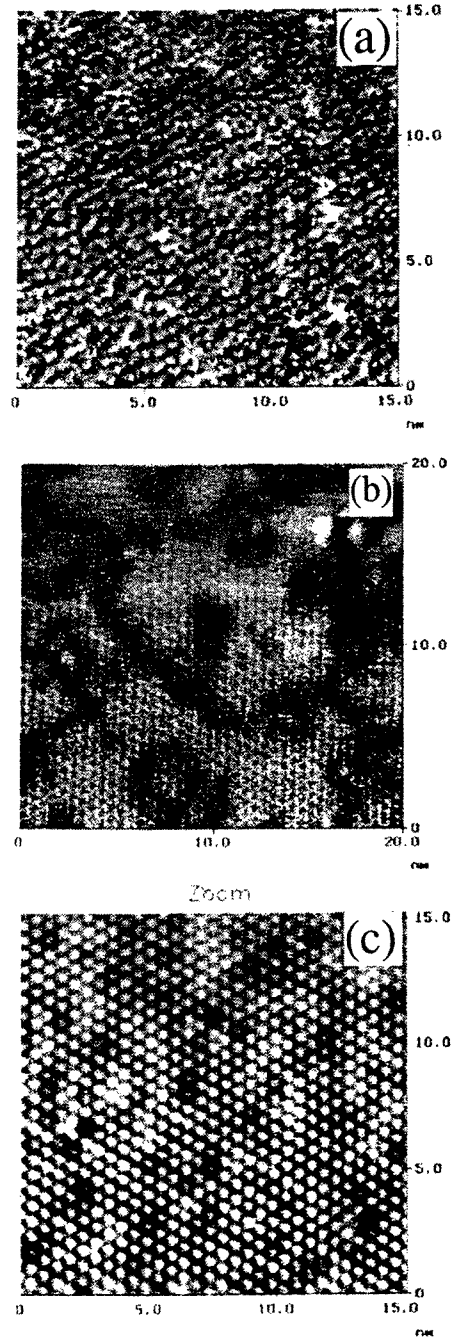

Fig. 5. In situ STM images of SCN on Pt(111) at (a) 0.9 V, (b) 0.3 V, (c) 0.1 V. The tip was biased -160 mV with respect to the Pt electrode.

segregated into islands-like features. In situ STM still revealed a (2×2) symmetry for the surface structure. These surface features were essentially unchanged between 0.7 and 0.3 V, although the quality of the STM imaging was markedly improved by the negative potential step. For example, Fig. 5(b), obtained at 0.1 V, shows islands of ordered (2×2) patterns. At 0.1 V the in situ STM discerned a long range well ordered (2×2) surface on Pt(111), except some lattice defects which appear 0.06 nm lower than the normal SCN protrusions. It is made clear that the (2×2) structure prevailing from 0.9 to 0.1 V contains 2 SCN per unit cell, which is consistent with the uhv results.[10] A better quality in situ STM

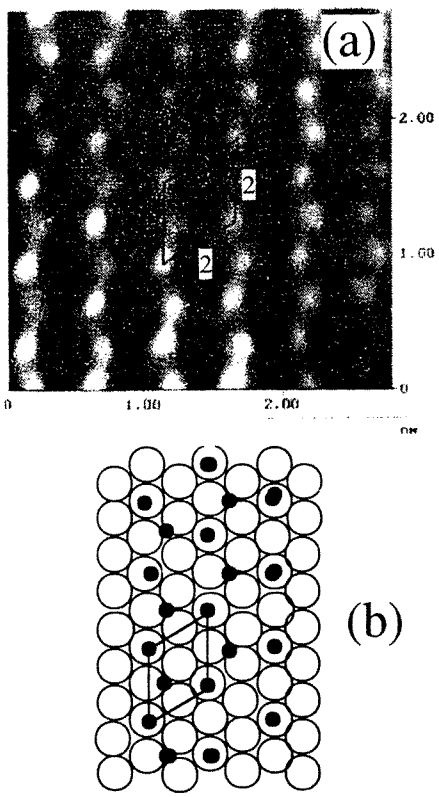

Fig. 6 An in situ STM atomic image of Pt(111)-(2x2)-2SCN structure (a) and a ball model (b).

atomic resolution of this (2×2) adlattice is shown in **Fig. 6(a)**. The corner atomic features seem to be brighter than the inside one. This STM result is in strong contrast to its normal p(2×2) appearance, found in Fig. 5. The different could more or less related to the arrangements of the SCN admolecules and the sharpness of the tip. the real space structure of the (2×2) pattern can be explained by the ball model in **Fig. 6(b)** which assign the four corner SCN to the atop sites while the inside SCN was placed on the three-fold sites. This model is consistent with the observed corrugations among the adsorbates at different registries.[22]

The surface changes by the negative potential stepping, as revealed by the in situ STM, is a reminiscent of those of adsorbed CN on Pt(111), whose coadsorbed K^+ cations of were substituted by protons, according to the reaction of Pt-SCN^-K^+ + $H_2O \rightarrow$ Pt-SCNH + K^+OH^-. No electron transfer is involved in this reaction so that no faradaic current emerged in the CV. Between 0.7 and 0.1 V the Pt surface was likely to contain both SCN^-K^+ and SCNH, which appear differently in the STM atomic resolutions. This K^+/H^+ replacing model indeed is in a better agreement with the reported HREEL results[20], showing the imminent prominence of the NH bending mode near 1400 cm^{-1} for more negative potential. Another scenario was proposed by the in situ IR results[23] which were interpreted as flipping SCN around to give NCS type surface species. This model does not seem to agree with our STM results which should have revealed the presence of two electronically different species at the negative end of potential window.

Conclusions

It is demonstrated that in situ STM imaging can be used to probe not only the detailed atomic structures of the specifically adsorbed anions at the IHP but also the coadsorbed cations at the OHP. In situ STM also revealed the crucial role of electrochemical potential in dominating the double layer structure. The population of the retained cations could be diminished by the replacement of hydronium cations.

Acknowledgment

We thank the ERATO project for financial support.

References:

(1) For a recent review, see: Siegenthaler, H. In *Scanning Tunneling Microscopy II*, Wiesendanger, R.; Guntherodt, H.-J., Eds.; Springer-Verlag, **1992**; pp 7-49.

(2) Yau, S.-L.; Vitus, C. M.; Schardt, B. C. *J. Am. Chem. Soc.* **1990**, *112*, 3677.

(3) Sugita, S.; Abe, T.; Itaya, K. *J. Phys. Chem.* **1993**, *97*, 8780.

(4) Tanaka, S.; Yau, S.-L.; Itaya, K. *J. Electroanal. Chem.* **1995**, in press.

(5) Funtikov, A. M., Linke, U., Stimming, U., Vogel, R. *Surf. Sic.* **1995**, *324*, L343.

(6) Wan, L.-J.; Yau, S.-L.;Itaya, K. *J. Phys. Chem.* **1995**, *99*, 9507.

(7) Bard, A. J.; Abruna, H. D.; Chidsey, C. E.; Faulkner, L. R.; Feldberg, S. W.;Itaya, K.; Majeda, M.;Melroy, O.;Murray. R. W.;Porter, M. D.; Sorriaga, M. P.; White, H. S. *J. Phys. Chem.* **1993**, *97*, 7147.

(8) Stickney, J. L.; Rosasco, S. D.; Salaita, G. N.; Hubbard, A. T. *Langmuir* **1985**, *1*, 66.

(9) Rosasco, S. D.; Stickney, J. L.; Salaita, G. N.; Frank, D. G.; Katekaru, J. Y.; Schardt, B. C.; Soriaga, M. P.; Stern, D. A.; Hubbard, A. T. *J. Electroanal. Chem.* **1983**, *188*, 95.

(10) Frank, D. G.; ; Katekaru, J. Y.; Rosasco, S. D.; Salaita, G. N.; Schardt, B. C.; Soriaga, M. P.; Stern, D. A.; Stickney, J. L.; Hubbard, A. T. *Langmuir* **1985**, *1*, 587.

(11) Kitamura, F.; Takahashi, M.; Ito, M. *Chem. Phys. Lett.* **1986**, *130*, 181.

(12) Kawashima, H.; Ikezawa, Y.; Takamura, T.*J. Electroanal. Chem.* **1991**, *317*, 257.

(13) Paulissen, V. B.; Korzeniewski, C. *J. Phys. Chem.* **1992**, *96*, 4563.

(14) Kim, C. K.; Korzeniewski, C. *J. Phys. Chem.* **1993**, *97*, 9784.

(15) Guyot-Sionnest, P.; Tadjeddine, A. *Chem. Phys. Lett.* **1990**, *172*, 341.

(16) Itaya, K.; Sugawara, S.; Sashikata, K.; Furuya, N. *J. Vac. Sci. Tech.* **1990**, *A8*, 515.

(17) Clavilier, J.; Rodes, A.; El Achi, K.; Zamakhchari, M. A. *J. Chim. Phys.* **1991**, *88*, 1291.

(18) Wanger, F. T.; Ross, P. N. *J. Electroanal. Chem.* **1988**, *250*, 301.

(19) Morallon, E.; Vazquez, J.; Aldaz, A. *J. Electroanal. Chem.* **1992**, *334*.

(20) Cao, E. Y.; Gao, P.; Gui, J. Y.; Lu, F.; Stern, D. A.; and Authur, A. T., *J Electroanal. Chem.* **1992**, *339*, 311.

(21) Kim, Y.G.; Yau, S.L.; Itaya, K. *J. Am. Chem. Soc.* submitted.

(22) Schardt, B.C.; Yau, S.L.; Rinaldi, F. *Science* **1989**, *243*, 1050.

(23) Ashley, K.; Samant, M.G.; Seki, H.; Philpott, M.R. *J. Electroanal. Chem.* **1989**, *270*, 349.